

# THE SYNTHESIS OF SOUND FIGURES

Karim Helwani · Sascha Spors · Herbert Buchner

**Abstract** In this paper we discuss a novel technique to control the spatial distribution of sound level within a synthesized sound field. The problem is formulated by separating the sound field into regions with high acoustic level, so-called bright regions, and zones with low acoustic level (zones of quiet) by time independent virtual boundaries. This way, the propagating sound field obtains a static spatial shape, which we call sound figure. This problem is treated with a generic approach for creating sound figures. We give an analytic solution to the problem and highlight, how our findings can be applied using established sound field synthesis techniques. We furthermore show the limitations of our approach, provide simulation results to prove the concept and discuss some application areas.

**Keywords** Multichannel sound reproduction · Sound field synthesis · Quiet zones · Sound figures

## 1 Introduction

Advanced multichannel sound reproduction techniques synthesize a sound scene for a large listening area. Most prominent examples of analytical techniques are Wave Field Synthesis (WFS) [5] and near-field compensated higher order Ambisonics (NFC-HOA) [11]. Here, the physical synthesis of a sound field within a spatially extended region of control  $\Lambda$  with

---

K. Helwani

Quality and Usability Lab, Telekom Innovation Laboratories, Technische Universität Berlin  
Ernst-Reuter-Platz 7, 10587 Berlin  
Tel.: +49 30 8353-58224  
Fax: +49 30 8353-58409  
E-mail: karim.helwani@telekom.de

S. Spors

Institut für Nachrichtentechnik, Universität Rostock  
Richard-Wagner-Str. 31, 18119 Rostock/Warnemünde

H. Buchner

Machine Learning Group, Technische Universität Berlin  
Franklinstr. 28/29, 10587 Berlin

This article is published in Multidim Syst Sign Process, April 2014, Volume 25, Issue 2, pp 379-403 and the final publication is available at [link.springer.com](http://link.springer.com)

the boundary  $\Omega_\Lambda$  is considered. The region of control is included in the domain  $S$  bounded by a distribution of secondary sources  $\Omega_S$ , where the term secondary source represents an abstract concept of a spatially continuous sound source, in the discrete case a secondary source refers to a loudspeaker. In figure 1 the synthesis setup is illustrated with the three relevant boundaries  $\Omega_S$  for the distribution of the secondary sources,  $\Omega_\Lambda$  for the boundary of the control region, and (as we will see later in this paper)  $\Omega_D$ , the boundary on which the sound figure is desired to be synthesized.

The concept of WFS is based on the Kirchhoff-Helmholtz integral [31]. This states that at any listening point within the source-free listening area  $\Omega_S$  the sound pressure is uniquely determined if both the sound pressure and its gradient are known on the boundary enclosing this area. Hence, in WFS the boundary  $\Omega_\Lambda$  and  $\Omega_S$  coincide.

NFC-HOA aims at an explicit solution of the wave equation, typically with Dirichlet boundary conditions [13] using orthogonal representations of the respective sound fields.

A goal of some recent work [1,8,21,28] was to achieve spatial selectivity of a synthesized sound field by defining closed regions with low acoustic level, so-called zones of quiet or *quiet zones*, in the listening area. For instance, the technique of acoustic contrast control [8,28] addresses maximum ratio of the acoustic energy in a region (its brightness) to the input energy under the constraint of maximizing the contrast between the bright zone and the quiet zone. The approach aims at finding an optimal solution at selected points in the listening area. Hence, the optimization will converge to locally optimal solutions. In [1] an approach for creating zones of quiet with circular loudspeaker arrays is described. The authors propose using higher order spherical harmonics to cancel the undesirable effects of the lower order harmonics of the desired sound field in the zone of quiet. This approach cannot be applied for arrays with other geometries than circular ones. Moreover, the boundaries of the resulting quiet zone have to be circular. In [21] the synthesis of sound fields with distributed modal constraints is considered. Unfortunately, the author in [21] does not provide a discussion on the limits of the presented approach or a time domain treatment of the underlying problem.

In this paper we discuss the synthesis of a desired spatial sound field with quiet zones having arbitrary predefined shape. In contrast to the Chladni figures [27] that also define spatial structures of sound fields in bounded resonant bodies, we are not interested in the interference patterns of standing waves but rather in the simultaneous synthesis of time independent spatial functions with traveling sound fields.

Moreover, we show in this paper how the obtained results can be applied with piecewise linear arrays which are of great interest from a practical point of view.

The potential applications of such a technique are manifold. Besides possible artistic applications, it is often desired to provide the possibility of spatially selective sound in terms of providing undisturbed communication. E.g., in a hands-free full-duplex communication system it is desired to prevent acoustic echoes. This can be achieved by creating a quiet zone in the region where the microphones are positioned [18]. Another application can be the hands-free communication in public places where it is desired to supply a diversity of uninterfered contents.

The paper proceeds as follows: In section 2 we briefly review the theory of the sound field synthesis and introduce the notation. In section 3 which should be considered as the central part of this paper, we introduce the mathematical formulation for the synthesis of sound figures, highlight the conditions for the synthesis of sound fields with spatial struc-

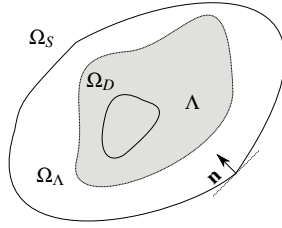


**Fig. 1** Geometry of the posed problem in the 2-dimensional case.  $\Omega_S$  denotes the distribution of the secondary sources,  $\Omega_\Lambda$  the boundary of the control region, and  $\Omega_D$  is the boundary on which the figure is desired to be synthesized.

ture, and derive an analytical solution. In section 4, we show, how to apply the developed synthesis approach to the synthesis of closed zones of quiet. Section 5 describes the synthesis using planar and linear arrays. Section 6 provides a discussion of some practical aspects and simulations to validate our concept and to emphasize the practical limits.

## 2 Synthesis of Sound Fields

Sound field synthesis techniques control the pressure profile on the boundary  $\Omega_S$  in order to synthesize a desired sound field in the domain bounded by  $\Omega_\Lambda$ , that we will denote by  $\Lambda$  throughout this paper. See Fig. 1. (We use the term *domain* as a generalization for a volume or an area depending on the dimensionality of the problem).

Furthermore, as detailed later in Sect. 3, the third boundary  $\Omega_D$  in Fig. 1 will be used for the definition of a sound figure within the synthesized sound field. The technique of wave field synthesis [5] is based on the Kirchhoff-Helmholtz integral. This states that the pressure  $P(\mathbf{x}, \omega)$  at any point  $\mathbf{x}$  inside a domain which is bounded by a closed manifold<sup>1</sup>  $\Omega_S$  is uniquely given by the pressure and velocity on the bounding manifold. In WFS the boundary of the control region  $\Omega_\Lambda$  is identical with the boundary defined by the secondary source distribution  $\Omega_S$ . The Kirchhoff-Helmholtz integral reads [34]

$$P(\mathbf{x}, \omega) = \oint_{\Omega_S} \left( P(\mathbf{x}_0, \omega) \cdot \frac{\partial}{\partial \mathbf{n}} G(\mathbf{x}|\mathbf{x}_0, \omega) - G(\mathbf{x}|\mathbf{x}_0, \omega) \cdot \frac{\partial}{\partial \mathbf{n}} P(\mathbf{x}_0, \omega) \right) d\mathbf{x}_0, \quad (1)$$

with

$$\frac{\partial}{\partial \mathbf{n}} P(\mathbf{x}_0, \omega) = \langle \mathbf{n}, \nabla P(\mathbf{x}_0, \omega) \rangle, \quad (2)$$

where  $\mathbf{n}$  denotes the inwards pointing normal vector on  $\Omega_S$ ,  $\frac{\partial}{\partial \mathbf{n}}$  the directional gradient taken in direction  $\mathbf{n}$ , and  $G(\mathbf{x}|\mathbf{x}_0, \omega)$  corresponds to the Green's function which is the solution of the inhomogeneous wave equation. Under free-field conditions, the Green's function describes a monopole source. In this paper we use the term secondary monopole sources for a distribution of monopole sources on  $\Omega_S$ . The directional gradient of the Green's function under free-field conditions can be seen as a dipole source. In a practical realization it is desirable to synthesize the sound field using only monopole sources located on  $\Omega_S$  since they can be approximated by loudspeakers. It can be shown that neglecting the dipole sources

<sup>1</sup> A manifold of dimension  $n$  is a topological space that resembles an  $n$ -dimensional Euclidean space in a neighborhood of each point [7].

in the synthesis process generates a soundfield outside the region bounded by  $\Omega_S$  however, inside  $\Omega_S$  the degradation of the synthesis can be reduced to a reasonable level by using a secondary source selection criterion [29] that is motivated by a high-frequency approximation as shown in [35]. This is briefly reviewed in the following. After eliminating the dipole secondary sources the synthesis equation (1) reads [31]

$$P(\mathbf{x}, \omega) \approx \oint_{\Omega_S} \underbrace{-2a(\mathbf{x}_0) \frac{\partial}{\partial \mathbf{n}} P(\mathbf{x}_0, \omega)}_{:=D(\mathbf{x}_0, \omega)} G(\mathbf{x}|\mathbf{x}_0, \omega) d\mathbf{x}_0, \quad (3)$$

where  $a(\mathbf{x}_0)$  is a window function corresponding to the selection criterion

$$a(\mathbf{x}_0) = \begin{cases} 1, & \text{if } \langle \mathbf{I}_S(\mathbf{x}_0, \omega), \mathbf{n}(\mathbf{x}_0) \rangle > 0, \\ 0, & \text{otherwise.} \end{cases} \quad (4)$$

Here,  $\mathbf{I}_S(\mathbf{x}_0, \omega)$  corresponds to the averaged acoustic intensity vector as introduced in [29].  $D(\mathbf{x}_0, \omega)|_{\mathbf{x}_0 \in \Omega_S}$  denotes the frequency dependent weighting function which is typically called driving function of the secondary source distribution.

As alternative to WFS, in the NFC-HOA literature, e.g., in [12, 14], the sound reproduction problem is considered as finding a solution of the wave equation with respect to a Dirichlet boundary condition. The problem is well posed and the sound field within  $\Lambda$  is uniquely defined by the pressure profile on  $\Omega_\Lambda$  for a given frequency  $\omega$  if and only if  $\omega$  does not correspond to a Dirichlet eigenvalue.

For the synthesis of a desired sound field in  $\Lambda$  one uses the equivalent integral equation to the wave equation with the Dirichlet boundary condition [12]. The resulting, so-called, Fredholm integral equation of the first kind is of the form [3]:

$$P(\mathbf{x}, \omega) = \oint_{\Omega_S} D(\mathbf{x}_0, \omega) G(\mathbf{x}|\mathbf{x}_0, \omega) d\mathbf{x}_0. \quad (5)$$

### 3 Analytical Solution to the Synthesis of Sound Figures

In this section, we develop the mathematical description for the synthesis of sound figures. Furthermore, we discuss the conditions for the existence of a solution. Obviously, such a discussion has also implications on the possible practical implementations. Furthermore, we derive an analytic solution.

#### 3.1 Problem Formulation

The term *sound figure* denotes a spatio-temporal distribution  $d_{\omega_0}(\mathbf{x}, t)$ , whose spatial components are time independent and can be represented as a given continuous spatial function  $f(\mathbf{x})$  on a predefined manifold  $\Omega_D$  (located within  $\Omega_S$  and  $\Omega_\Lambda$ , see Fig. 1). The temporal component of a sound figure  $d_{\omega_0}(\mathbf{x}, t)$  can be represented as harmonic oscillation with the frequency  $\omega_0$  as  $e^{i\omega_0 t}$ . Hence, we write:

$$d_{\omega_0}(\mathbf{x}, t) = f(\mathbf{x}) e^{i\omega_0 t} \Big|_{\mathbf{x} \in \Omega_D}, \quad (6)$$

where  $i$  denotes the imaginary unit with  $i^2 := -1$ . As will become apparent, such a function can define the boundary of a zone of quiet in a synthesized sound field.

Giving a closed non-overlapping manifold  $\Omega_D^2$ , we outline how to synthesize a desired sound figure on this manifold, highlighting the conditions for the synthesis.

The considered sound field synthesis problem is related to solving the wave equation with respect to boundary conditions that we give in the following.

The wave equation can be formulated in the frequency domain by considering its steady state solutions yielding the Helmholtz equation [34]

$$\Delta P(\mathbf{x}, \omega) + \left(\frac{\omega}{c}\right)^2 P(\mathbf{x}, \omega) = 0, \quad (7)$$

with  $c$  denoting the speed of sound. The boundary conditions from (6) are

$$P(\mathbf{x}, \omega)|_{\mathbf{x} \in \Omega_D} = f(\mathbf{x}), \quad \frac{\partial P(\mathbf{x}, \omega)}{\partial \mathbf{n}} \Big|_{\mathbf{x} \in \Omega_D} = f'(\mathbf{x}), \quad (8)$$

where  $'$  denotes the spatial derivative. Note that the soundfield  $P(\mathbf{x}, \omega)$  at the boundary  $\Omega_D$  is constant for all temporal frequencies  $\omega$  and given by the spatial function  $f(\mathbf{x})$ . Therefore, the soundfield in the time domain  $p(\mathbf{x}, t)$  is an impulse at the boundary  $\Omega_D$ . Due to the discontinuity of the pressure along the normal direction  $\mathbf{n}$  w.r.t.  $\Omega_D$  the second boundary condition is usually split up into an exterior and an interior condition. The equivalent integral equation to the wave equation with respect to these two boundary conditions is a Fredholm equation of second kind [33]. The integral equation corresponding to the interior boundary condition reads

$$P_0(\mathbf{x}, \omega) = P^-(\mathbf{x}, \omega) - k_n^2 \oint_{\Omega_D} P(\mathbf{x}_0, \omega) G(\mathbf{x}|\mathbf{x}_0, \omega) d\mathbf{x}_0, \quad (9)$$

with  $P_0(\mathbf{x}, \omega)$  denoting a predefined sound field that is desired besides the sound figure,  $k_n \in \mathbb{R}$  denoting the discrete eigenvalues of the wave equation under the two boundary conditions,  $n \in \mathbb{N}$  standing for the eigenvalue index, and  $P^-(\mathbf{x}, \omega)$  denotes the sound field inside the region bounded by  $\Omega_D$ . Analogously, the exterior boundary condition corresponds to

$$P_0(\mathbf{x}, \omega) = P^+(\mathbf{x}, \omega) + k_n^2 \oint_{\Omega_D} P(\mathbf{x}_0, \omega) G(\mathbf{x}|\mathbf{x}_0, \omega) d\mathbf{x}_0, \quad (10)$$

where  $P^+(\mathbf{x}, \omega)$  denotes the sound field outside the region bounded by  $\Omega_D$ .

A sufficient condition for the existence of a solution for this integral equation is the orthogonality of  $P(\mathbf{x})$  to the independent solutions of the adjoint operator [10]. In next section we give a constructive proof of the existence of a solution for our special problem.

## 3.2 Conditions for the Synthesis of Sound Figures

### 3.2.1 Preliminary Considerations

To illustrate the properties of the solution of the Helmholtz equation, let us for ease of presentation consider the subspace spanned by the eigenfunctions solving the wave equation in

<sup>2</sup> A non-overlapping manifold  $\Omega$  does not exhibit any nodes. This property is necessary for defining differential operators on  $\Omega$ .

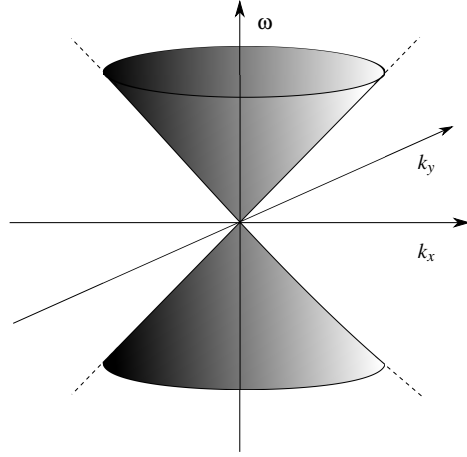


**Fig. 2** Manifold on which the eigenvalues corresponding to the solutions of the homogeneous wave equation are located on [25,24].

the 2-dimensional case corresponding to real eigenvalues of the Laplace operator in Cartesian coordinates. These are given as [34]:

$$P(\omega, \mathbf{x}) = A(\omega)e^{i\mathbf{k}\mathbf{x}^T}. \quad (11)$$

This function represents a general solution of the Helmholtz equation in Cartesian coordinates, where  $A(\omega)$  denotes the frequency dependent weighting factor,  $\mathbf{k}$  is the wave vector consisting in the 2-dimensional case of the two components  $\mathbf{k} := [k_x, k_y]$ , and  $\mathbf{x} := [x, y]$  the position. Introducing (11) to (7) results in

$$\|\mathbf{k}\| = \frac{\omega}{c} := k. \quad (12)$$

Hence, the Helmholtz equation reveals a dependency between the spatial and temporal components of the harmonic solutions of the wave equation. This relation is expressed by (12) and is known as the dispersion relation [24,34,25]. In Fig. 2 we show the manifolds on which the eigenvalues corresponding to the solutions of the Helmholtz equation are located on. The components  $[k_x, k_y]$  are depicted in the horizontal plane and the temporal frequency  $\omega$  on the vertical axis of a Cartesian coordinate system. The manifold of the solutions represents surface of a double cone. Hence, the solutions of the wave equation for a single temporal frequency lie on a circle with radius  $k$ .

It can be shown, that the validity of (12) can be extended to different coordinate systems in  $\mathbb{R}^M$ , with  $1 \leq M \leq 3$ , in which the Laplace operator can be separated into  $M$  variables. The Helmholtz equation poses a dependency between the spatial components of its non-trivial solutions. It is not obvious if it is possible to obtain solutions of the form of (6) on a manifold of the dimensionality  $M - 1$  which is embedded in  $\mathbb{R}^M$ . Therefore, we will discuss in the following how to obtain such solutions of the homogeneous and inhomogeneous wave equation.

### 3.2.2 Functions on Closed One-Dimensional Manifolds as Solutions of the Homogeneous Wave Equation

For ease of presentation we consider in this subsection only 1-dimensional manifolds embedded in  $\mathbb{R}^2$ , the generalization to 2-dimensional manifolds can be done in a straightforward manner.

The wave equation can be solved using the technique of separation of variables in suitable coordinate systems, such as cylindrical or spherical coordinates. The solutions of the two-dimensional wave equation  $\psi_n(\mathbf{x})$  in cylindrical coordinates span a subspace which we denote by

$$\mathcal{R}_\Psi := \left\{ f(\mathbf{x}) \mid f(\mathbf{x}) = \sum_{n=0}^{\infty} a_n \psi_n(\mathbf{x}), \mathbf{x} \in \mathbb{R}^2, a_n \in \mathbb{R} \right\}. \quad (13)$$

The eigenfunctions  $\psi_n(x, y)$  have spatial dimensionality of one since the solutions of the wave equation have to fulfill the dispersion relation. For fixed  $\omega$  this states a dependency of the two spatial components of a traveling wave.

Suppose there exists a coordinate system for the Euclidean space with a locally invertible transformation from a set of Cartesian coordinates,  $\Xi : (x, y) \rightarrow (\xi_1, \xi_2)$ , such that a parametrization of the manifold  $\Omega_D$  is given as

$$\forall (\xi_1, \xi_2) \in \Omega_D. \quad \xi_2 = \text{const}. \quad (14)$$

The Laplace-Beltrami operator<sup>3</sup> in this coordinate system, so-called curvilinear coordinates, along  $\xi_1$  has a discrete spectrum since the coordinates are defined by a closed manifold which is a compact boundaryless manifold [26]. Now assume we have the eigenfunctions  $\phi_n(\xi_1, \xi_2)$  of the Laplace-Beltrami operator defined on the manifold  $\Omega_D$ . Since  $\Omega_D$  is compact, the set of eigenfunctions  $\{\phi_n(\xi_1, \xi_2) \mid n \in \mathbb{N}, (\xi_1, \xi_2) \in \Omega_D\}$  defines a complete orthogonal basis for continuous functions defined on  $\Omega_D$ . We term the subspace spanned by these basis functions as  $\mathcal{R}_\Phi$ . Let us assume the function to be synthesized is spanned by the subspace  $\mathcal{R}_{\Phi_0} \subseteq \mathcal{R}_\Phi$ .

A sound figure can be seen as a solution of the Helmholtz equation if and only if it is included in the range

$$\mathcal{R}_{\Psi_{\Omega_D}} := \left\{ f(\mathbf{x}) \mid f(\mathbf{x}) = \sum_{n=0}^{\infty} a_n \psi_n(\mathbf{x}), \mathbf{x} \in \Omega_D, a_n \in \mathbb{R} \right\}. \quad (15)$$

Hence, we obtain the first condition that has to be fulfilled for perfectly synthesizing a continuous function on  $\Omega_D$

$$\mathcal{R}_{\Phi_0} \cap \mathcal{R}_{\Psi_{\Omega_D}} = \mathcal{R}_{\Phi_0}. \quad (16)$$

In other words, the subspace in which the sound figure is embedded has to be a subspace of the space spanned by the eigenfunctions of the Helmholtz equation.

<sup>3</sup> In differential geometry, the Laplace operator can be generalized to operate on functions defined on surfaces in Euclidean space and, more generally, on Riemannian and pseudo-Riemannian manifolds. This more general operator goes by the name Laplace-Beltrami operator. The Laplace-Beltrami operator, like the Laplacian, is the divergence of the gradient.

### 3.2.3 Functions on Closed One-Dimensional Manifolds as Solutions of the Inhomogeneous Wave Equation

In the following we consider the synthesis of sound figures that fulfill the above discussed condition by considering the inhomogeneous wave equation.

Suppose we desire to synthesize a continuous function on a closed and non-overlapping manifold  $\Omega_D$  embedded in a region bounded by a closed and non-overlapping secondary source distribution on  $\Omega_S$ , see Fig. 1.

One prominent technique of solving the Helmholtz equation with one boundary condition is by formulating the equivalent integral equation. It can be shown that the resulting adjoint integral operator, the so-called Fredholm Operator is compact [15], and so its spectrum is discrete. Hence, diagonalizing the Fredholm operator in (5) is usually achieved by decomposing the operator into orthogonal components [13, 15, 23]. Unfortunately, analytical expressions for the eigenfunctions of the Fredholm operator are known only for few geometries. Moreover, the eigenfunctions of this operator depend on the relative position of  $\Omega_D$  in  $\Omega_S$ , hence, a change of the position of the desired zone of quiet could result in changing the eigenfunctions. In this study we are interested in the boundaries of both, the secondary source distribution as well as the boundary defined by the desired sound figure. The assumption that these boundaries are constant due to the predefined geometry of the array and the zone of quiet does not pose a strong constraint on the fixed position of the zone of quiet. Therefore, we introduce two transformations corresponding to the bases defined by the eigenfunctions of the Laplace-Beltrami operator on the source manifold  $\Omega_S$  as well as on the destination manifold  $\Omega_D$ .

We define a transformation of the pressure on the destination manifold into the domain defined by the eigenfunctions of the Laplace-Beltrami operator of  $\Omega_D$  by

$$\tilde{P}_n(\omega) = \oint_{\Omega_D} P(\mathbf{x}, \omega) \phi_n^*(\mathbf{x}, \omega) d\mathbf{x}, \quad (17)$$

where we introduce the notation  $\tilde{\cdot}$  to denote a spatial transformation. The corresponding left transformation of the Green's function is defined by

$$\tilde{G}_n(\mathbf{x}_0, \omega) = \oint_{\Omega_D} G(\mathbf{x}|\mathbf{x}_0, \omega) \phi_n^*(\mathbf{x}, \omega) d\mathbf{x}. \quad (18)$$

Here we assume that the Green's function does not exhibit singularities along  $\Omega_D$ . Analogously, we define a transformation of the pressure profile on the source manifold into the domain defined by the eigenfunctions of the Laplace-Beltrami operator of  $\Omega_S$ ,  $\Upsilon(\mathbf{x})$  by

$$\tilde{D}_m(\omega) = \oint_{\Omega_S} D(\mathbf{x}_0, \omega) \Upsilon_m^*(\mathbf{x}_0, \omega) d\mathbf{x}_0. \quad (19)$$

The corresponding right transformation of the Green's function reads

$$\tilde{\tilde{G}}_{n,m}(\omega) = \oint_{\Omega_S} \tilde{G}_n(\mathbf{x}_0, \omega) \Upsilon_m^*(\mathbf{x}_0, \omega) d\mathbf{x}_0, \quad (20)$$

where the notation  $\tilde{\tilde{\cdot}}$  emphasizes the double-sided transformation with respect to two boundaries. Again we assumed in Eq. (20) that the Green's function does not exhibit singularities along  $\Omega_S$ .

Assuming that the function  $f(\mathbf{x})$  to be synthesized on the manifold  $\Omega_D$  can be approximated

with the eigenfunctions  $\phi_n$  up to the order  $N$  and we aim at approximating the driving function  $D(\mathbf{x}_0, \omega)$  using a limited number of eigenfunctions  $\Upsilon_m$  with  $m \leq M$  we can set up a system of equations

$$\tilde{\mathbf{P}}(\omega) = \tilde{\mathbf{G}}(\omega)\tilde{\mathbf{D}}(\omega), \quad (21)$$

with

$$\tilde{\mathbf{G}}(\omega) := \begin{bmatrix} \tilde{G}_{1,1}(\omega) & \dots & \tilde{G}_{1,M}(\omega) \\ \tilde{G}_{2,1}(\omega) & \dots & \tilde{G}_{2,M}(\omega) \\ \vdots & \ddots & \vdots \\ \tilde{G}_{N,1}(\omega) & \dots & \tilde{G}_{N,M}(\omega) \end{bmatrix}, \quad (22)$$

where  $\tilde{\mathbf{D}}(\omega) = [\tilde{D}_1(\omega), \dots, \tilde{D}_M(\omega)]^T$  and  $\tilde{\mathbf{P}} = [\tilde{P}_1(\omega), \dots, \tilde{P}_N(\omega)]^T$ . If the resulting system of equations is square ( $N = M$ ), there exists a unique solution if and only if the eigenvalues of the equation system matrix do not degenerate. In the general case and for  $N \neq M$  the necessary and sufficient condition for the solvability of the  $N \times M$  system is that the left side is orthogonal to all linearly independent solutions of the adjoint homogeneous system [20]. Note the equivalence of this condition to the condition for the existence of a solution for the Fredholm integral equation of second kind [10].

A quasi-solution can be obtained using the least-squares optimization criterion and applying an appropriate regularization strategy [33].

### 3.2.4 Note on Discrete Distributions of Secondary Sources

In practical realizations the number of secondary sources is usually finite and the manifold  $\Omega_D$  is approximated by a finite set of points. Therefore, one might be interested in the discrete formulation of the Laplace-Beltrami operator. A common structure used for a geometrical approximation of manifolds embedded in the Euclidean space  $\mathbb{R}^M$  is a vertex graph which is in turn defined as the topology  $(V, E)$  [9, 19]. Hereby,  $V$  is a set of indices denoting the sampling points, with cardinality  $|V| = N$  (i.e., each index corresponds to a secondary source or to a measuring point on  $\Omega_D$ ).  $E$  is a set of pair of vertices and is symmetric. Typically, the set of edges is represented by a symmetric matrix, the so-called adjacency matrix [9]. On the so defined graph the discrete Laplace-Beltrami operator is given as

$$\mathbf{L} = \mathbf{C} - \mathbf{W} \quad (23)$$

with  $\mathbf{C} = \text{diag}\{\mathbf{c}\}$ ,  $\mathbf{c} = [c_1, \dots, c_i, \dots, c_N]$  and  $c_i = \sum_j w_{ij}$ .  $w_{ij}$  are local averaging coefficients. The computation of the averaging coefficients can be performed in different manners. For our considerations of two-dimensional synthesis using distributions of loudspeakers on 1-dimensional manifolds, the distance weights  $\forall (i, j) \in E$ ,  $w_{ij} := \frac{1}{\|\mathbf{x}_j - \mathbf{x}_i\|^2}$  offers a good approximation [9]. Where  $\mathbf{x}_i$  denotes the coordinates of the  $i$ -th sampling point.

Note that in the spatially discrete case the computation of the subspace intersection can be done in an efficient way based on determining the angle between the subspaces [16].

Moreover, the spatial spectrum of a signal in the discrete case is frequency dependent. As first approximation a spatial discretization leads to spectral repetitions depending on the discretization scheme. Above a given temporal frequency the spectral components may overlap. Hence, the spatial spectral transformation becomes ill-conditioned and a reconstruction of the spatio-temporal signal from its spectrum is in general not possible any more.

#### 4 Synthesis of Closed Zones of Quiet

The concept of synthesizing sound figures on one- or two-dimensional manifolds can be used to create bounded zones of quiet. The idea is to synthesize a pressure function on the manifold  $\Omega_D$  that is equivalent to the pressure of a scattered field by a rigid boundary coincident with  $\Omega_D$ . The sound field at a rigid boundary has to fulfill the condition

$$\left. \frac{\partial P(\mathbf{x}, \omega)}{\partial \mathbf{n}} \right|_{\mathbf{x} \in \Omega_D} = \mathbf{0}, \quad (24)$$

which is known as the Neumann boundary condition. Note that this can be considered as a special case of the Robin problem [17]. In this paper we restrict our considerations to the rigid boundary condition.

In the following we outline how to derive the driving functions and give an example of synthesizing a circular zone of quiet within a plane wave as depicted in Fig. 3. The sound figure to be synthesized is a function of pressure on  $\Omega_D$  which is given by scattering a plane wave on a closed rigid object which is infinite in the  $z$ -direction. Since the boundary is rigid the directional derivative of the transformed overall pressure on the considered manifold  $\Omega_D$  should be identical to zero,

$$\sum_n \frac{\partial}{\partial \mathbf{n}} (\tilde{P}_{\text{inc},n} + \tilde{P}_{\text{scat},n}) \phi_n(\mathbf{x}) \Big|_{\mathbf{x} \in \Omega_D} = \mathbf{0}, \quad (25)$$

where  $\tilde{P}_{\text{inc},n}$  and  $\tilde{P}_{\text{scat},n}$  denote the transformed incident and scattered plane waves on  $\Omega_D$ , respectively. Due to orthogonality and completeness of the eigenfunctions, each term in this sum should be zero so that

$$\frac{\partial}{\partial \mathbf{n}} \tilde{P}_{\text{scat},n} = - \frac{\partial}{\partial \mathbf{n}} \tilde{P}_{\text{inc},n}, \quad \forall n \in \mathbb{N}. \quad (26)$$

Once the directional gradient is given, the pressure can be computed straightforwardly by exploiting the linear relation between them by employing the Euler equation. Substituting this into (21) results in a system of equations involving the unknown driving functions. Ideally, the system of equations is quadratic ( $N = M$ ) and well conditioned or fulfills the condition discussed in Sect. 3.2.3. Otherwise, an approximate solution can be obtained by formulating a least-squares optimization problem and incorporating prior knowledge using the Lagrange multiplier formalism to regularize the ill-conditioned problem. A prominent regularization approach is the so-called Tikhonov regularization which constrains the  $\ell_2$ -norm of the vector-valued solution of the optimization problem [33].

In the following we give as an example the driving functions for a circular zone of quiet. The sound figure to be synthesized is a function of pressure on a circle which is given as a cross section of the infinite rigid cylinder at  $z = 0$  with the radius  $a$ . The desired pressure on this circle  $\Omega_D$  is given by scattering a plane wave on the rigid cylinder, see Fig. 3.

##### *Approximation of the Driving Functions Based on the Kirchhoff-Helmholtz Integral*

The synthesis of a scattered field can be done using the WFS synthesis equation, (3). In a similar way as presented [30] for synthesizing the scattered field of a sound soft boundary, the synthesis process can be summarized by the following steps

- compute the directional gradient of the sound field of the virtual source scattered by a virtual object that encloses the local listening area  $\Omega_S$ ,

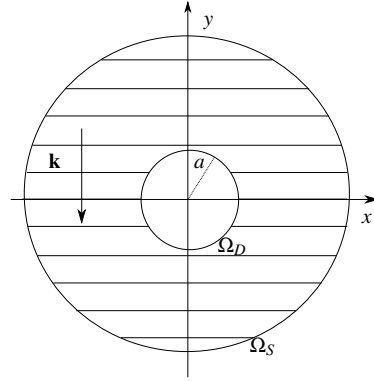


**Fig. 3** Geometry for creating a circular zone of quiet within a desired plane wave. The vertical arrow stands for the direction of incidence of the synthesized plane wave.

- time-reverse the computed sound field,
- select the required secondary sources,
- emit the time-reversed sound field by the active secondary sources, and
- in addition, emit the globally desired sound field (the desired sound field outside the zone of quiet).

#### Analytical Derivation of the Driving Functions

The eigenfunctions of the Laplace-Beltrami operator on the unit circle are exponential functions (Fourier basis). Hence, we set

$$\phi_n(\varphi) = e^{in\varphi}, \quad (27)$$

with  $\mathbf{x} = [x, y] = \|\mathbf{x}\|[\cos(\varphi), \sin(\varphi)]$ . Since  $\Omega_S$  is a circle with the same center as  $\Omega_D$ , see Fig. 3, we set

$$\Upsilon_n(\varphi_0) = e^{in\varphi_0}. \quad (28)$$

The scattered field on a cylinder of infinite length is given by [32]

$$P_{\text{scat}}(\mathbf{x}, \omega) = - \sum_{n=-\infty}^{\infty} i^n \left( \frac{J'_n(ka)H_n^{(2)}(k\|\mathbf{x}\|)}{H_n^{(2)'}(ka)} e^{in(\varphi-\varphi_s)} \right), \quad (29)$$

where  $\varphi_s$  denotes the angle of incidence of the plane wave,  $J_n(\cdot)$  the Bessel function of  $n$ -th order and  $H_n^{(2)}(\cdot)$  corresponds to the Hankel function of the second kind and  $n$ -th order, and the prime denotes the derivative with respect to the argument. Note that the scattered wave can be regarded as a time reversed version of the Fourier transformation of its complex conjugate function. Therefore, synthesizing the scattered part of the sound field has to incorporate a pre-delay to ensure the causality of the synthesis filters. The incident plane wave can be expressed as

$$P_{\text{inc}}(\mathbf{x}, \omega) = \sum_{n=-\infty}^{\infty} i^n J_n(k\|\mathbf{x}\|) e^{in(\varphi-\varphi_s)}. \quad (30)$$

Hence, the overall pressure is given by

$$P(\mathbf{x}, \omega) = \sum_{n=-\infty}^{\infty} i^n \left( J_n(k\|\mathbf{x}\|) - \frac{J'_n(ka)H_n^{(2)}(k\|\mathbf{x}\|)}{H_n^{(2)'}(ka)} \right) e^{in(\varphi-\varphi_s)}. \quad (31)$$

The transformation according to (17) offers the Fourier coefficients yields

$$\tilde{P}_n(\omega) = i^n \left( J_n(k\|\mathbf{x}\|) - \frac{J'_n(ka)H_n^{(2)}(k\|\mathbf{x}\|)}{H_n^{(2)'}(ka)} \right) e^{-in\varphi_s}. \quad (32)$$

The point source solution of the two-dimensional inhomogeneous wave equation is given by the Green's function: [34]

$$G_n(\mathbf{x}|\mathbf{x}_0) = \frac{i}{4} H_0^{(1)}(k\|\mathbf{x} - \mathbf{x}_0\|). \quad (33)$$

The Fourier series expansion of the Green's function reads

$$G(\mathbf{x}|\mathbf{x}_0) = \sum_{n=0}^{\infty} J_n(k\|\mathbf{x}\|) H_n^{(1)}(k\|\mathbf{x}_0\|) e^{in(\varphi-\varphi_0)}, \quad (34)$$

therefore, the left transformation according to (18) is given by

$$\tilde{G}_n(\mathbf{x}_0) = J_n(k\|\mathbf{x}\|) H_n^{(1)}(k\|\mathbf{x}_0\|) e^{-in\varphi_0}. \quad (35)$$

Since the Laplace-Beltrami operators for both manifolds  $\Omega_D$  and  $\Omega_S$  are identical, applying a right transformation reveals that the system matrix in (21) is diagonal. The expression for the left and right transformed Green's function is given according to (20)

$$\tilde{\tilde{G}}_{mn} = J_n(k\|\mathbf{x}\|) H_n^{(1)}(k\|\mathbf{x}_0\|). \quad (36)$$

Finally, the transformed driving functions are derived as

$$\tilde{D}_n = i^n \left( \frac{1}{H_n^{(1)}(k\|\mathbf{x}_0\|)} - \frac{J'_n(ka)H_n^{(2)}(k\|\mathbf{x}\|)}{J_n(k\|\mathbf{x}\|)H_n^{(1)}(k\|\mathbf{x}_0\|)H_n^{(2)'}(ka)} \right) e^{-in\varphi_s}. \quad (37)$$

In terms of illustrating the synthesis of a sound field with a closed zone of quiet we give a simulation result using a 100 element circular loudspeaker array of radius 1.45 m for synthesizing a plane wave with an angle of incidence of  $\varphi_s = \frac{\pi}{2}$  with a concentric circular zone of quiet with a radius of  $a = 30$  cm. In Fig. 4 the synthesized sound field and its level distribution is depicted at a frequency of 1 kHz. The time domain simulation is given in Fig. 5 and emphasizes the synthesis of the scattered part of the field with a suitably chosen predelay.

## 5 Linear Distribution of Secondary Sources as Limiting Case of a Closed Distribution

So far, we discussed the synthesis of closed zones of quiet using closed secondary source distributions. In the following we state which assumptions have to be made to consider the case of linear secondary source distributions as a specialization of the discussed results. Studying the linear case gives an intuitive illustration of the presented framework due to analogies to traditional and well known temporal signal processing techniques.

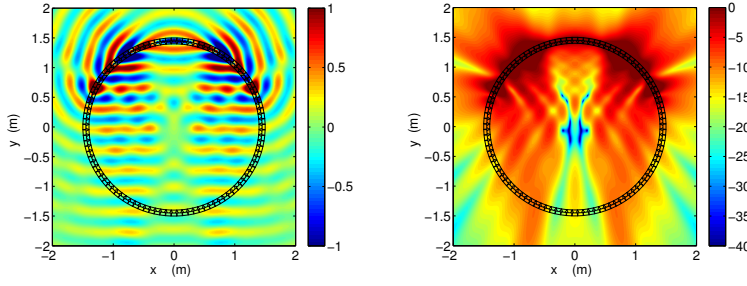


**Fig. 4** Simulated plane wave with a closed zone of quiet at 1000 Hz (left) and the achieved level distribution of the synthesized plane wave (right) in [dB] with a zone quiet of a radius of  $a=0.3$  m using an array with 100 loudspeakers on a radius of 1.45 m.

### 5.1 Linear Secondary Source Distributions

Specializing the Kirchhoff-Helmholtz integral to a linear secondary source distribution leads to the Rayleigh integrals [6]. Let us assume that the line  $\Omega_{S_0}$  in Fig. 6 coincides with the secondary source distribution. Let us imagine a closed continuation as a part of a circle with a radius  $r \rightarrow \infty$  with the center at  $A$ . We are interested in determining the sound pressure in  $A$  due to a virtual point source at  $B$  by measurements on  $\Omega_{S_0}$ . The contribution of the Kirchhoff-Helmholtz integral over  $\Omega_{S_1}$  to the pressure in  $A$  vanishes if  $r$  goes to infinity due to the Sommerfeld radiation condition [6]. Hence, the Kirchhoff-Helmholtz integral (1) may be replaced by [6]

$$P(\mathbf{x}, \omega) = \int_{-\infty}^{\infty} \left( P(\mathbf{x}_0, \omega) \cdot \frac{\partial}{\partial \mathbf{n}} G(\mathbf{x}|\mathbf{x}_0, \omega) - G(\mathbf{x}|\mathbf{x}_0, \omega) \cdot \frac{\partial}{\partial \mathbf{n}} P(\mathbf{x}_0, \omega) \right) d\mathbf{x}_0. \quad (38)$$

Analogously, to the case of a closed distribution of secondary sources one omits the summand with the dipole sources in (38).

By similar argumentation as shown above, the explicit synthesis equation (5) can be specialized to describe the synthesis process using a linear distribution of secondary sources [2].

$$P(\mathbf{x}, \omega) = \int_{-\infty}^{\infty} D(\mathbf{x}_0, \omega) G(\mathbf{x} - \mathbf{x}_0, \omega) d\mathbf{x}_0, \quad (39)$$

here again  $D(\mathbf{x}_0, \omega)$  denotes the driving function of the secondary sources. The secondary source distribution is assumed to be along the  $x$ -axis thus  $\mathbf{x}_0 = [x_0, 0, 0]$  and  $\mathbf{x} = [x, y_{\text{ref}}, 0]$  defines a reference line on which the reproduction should be perfect. The secondary sources are driven by the signal  $D(\mathbf{x}_0, \omega)$ .  $G(\mathbf{x} - \mathbf{x}_0, \omega)$  denotes the spatio-temporal transfer function from a secondary source located at  $\mathbf{x}_0$  to a point at  $\mathbf{x}$ .

### 5.2 Arrays with Convex Geometries as Linear Arrays

Linear and planar arrays can only synthesize wave fronts traveling into the target half space. E.g., with a planar array located in the  $x$ - $z$ -plane, i.e.,  $\mathbf{x}_0 = [x_0, 0, z_0]$  the synthesis is targeted to that part of the space which contains the positive  $y$ -axis. Hence, the synthesis of plane waves with such arrays is only possible for waves in one half of the wave number space.

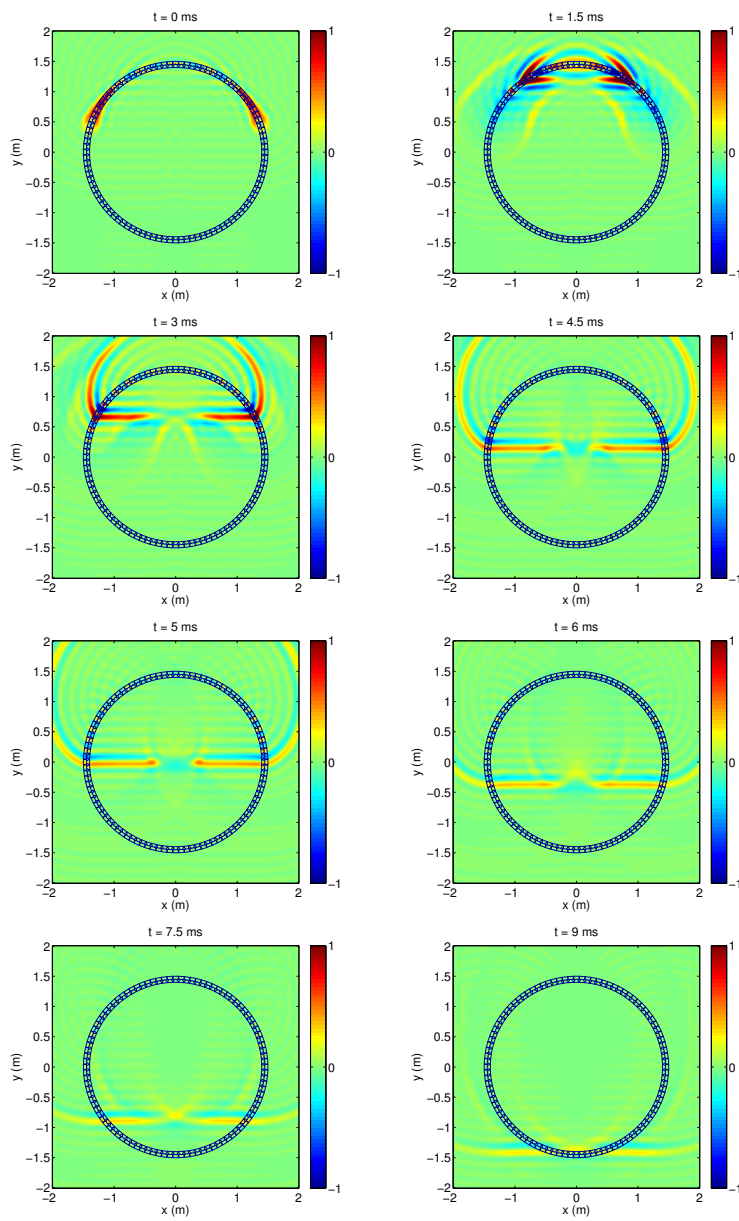


**Fig. 5** Time-domain simulation of a wave with a zone quiet of a radius of  $a = 0.3$  m using an array with 100 loudspeakers on a radius of 1.45 m.

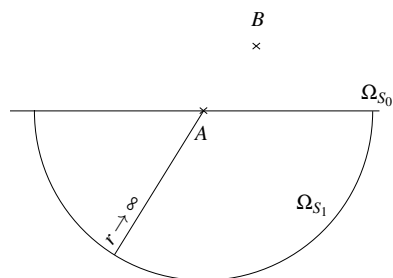


**Fig. 6** Illustration of the derivation of the Rayleigh integral equation [6].  $A$  stands for the center of the circle with  $r \rightarrow \infty$  that extends the linear array to a closed manifold, and  $B$  denotes the position of the virtual source.

This problem can be overcome and the synthesis can cover the entire wave number space if the used secondary source distribution encloses the target volume.

The theory of wave field synthesis makes a convexity assumption on the geometry of the enclosing distribution with respect to the target volume. Arbitrary convex secondary source distributions are usually treated as locally planar (linear). This approximation originates from the scattering theory and is known as Kirchhoff or physical optics approximation [4, 14] and holds for small wave lengths compared to the dimensions of the secondary source distribution. Moreover, employing this approximation requires a rule for secondary source selection. A secondary source is selected if the normal vector  $\mathbf{n}$  of the secondary source and the propagation direction of the plane wave  $\mathbf{n}_{pw}$  form an acute-angle [29]. A preferred two-dimensional secondary source distribution that encloses the target plane is the rectangular distribution. Theoretically, such a distribution is treated as a combination of two complementary convex distributions, each of them is approximated by two local linear distributions which can be treated by our consideration outlined in the previous subsection, see Fig. 7.

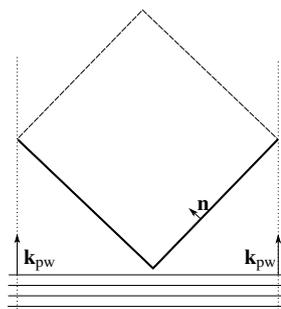


**Fig. 7** Secondary source selection for a virtual plane with propagation direction  $\mathbf{k}_{pw}$ . Bold solid lines indicate the active parts of secondary source distribution for the synthesis of the virtual plane wave.

### 5.3 Example of the Synthesis of Sound Figures on a Line Using Linear Arrays

In the case of an infinitely long linear distribution of secondary sources it is well known, that the eigenfunctions of the Laplace operator along one Cartesian coordinate are the exponential basis functions of the Fourier transform [34]. A common representation of sound fields using the Fourier basis is the  $k$ -space representation. As outlined in Sect. 3.2.1, monochromatic traveling waves at frequency  $\omega = kc$  can be represented as a circle with radius  $k$ , see Fig. 8 that results as a cross-section of the double cone in Fig. 2. We show exemplary the synthesis of a one-dimensional rectangular window as a sound figure using a linear array of loudspeakers in the eigenspace domain.

The choice of this example is motivated by the fact that reproducing zones of quiet nearby a desired sound field with linear secondary source distributions can be achieved by multiplying the desired wave field on a line which is parallel to the secondary source distribution and that we will call reference line with a rectangular window.

In terms of considering sound figures on a line as a special case of the discussed sound figures on closed manifolds we restrict our consideration on the periodic continuation of a desired spatially finite sound figure. Periodic one- or two-dimensional functions have a discrete spectrum and the eigenfunctions of these form the Fourier series basis. Hence, for a one dimensional function we can set for each temporal frequency

$$\Upsilon_n(x) = \phi_n(x) = \frac{1}{2\pi} e^{inx}. \quad (40)$$

A plane wave which propagates along the x-y-plane is given as

$$p(x, y, t) = e^{-i(k_{pw,x}x + k_{pw,y}y - \omega_{pw}t)}, \quad (41)$$

with  $[k_{pw,x} \ k_{pw,y}] = \frac{\omega_{pw}}{c} [\cos(\theta_{pw}) \ \sin(\theta_{pw})]$ , where  $\theta_{pw}$  denotes the propagation direction of the plane wave in the x-y-plane.

Performing a Fourier transformation with respect to time and space along the x-axis leads to

$$\tilde{P}(k_x, y, \omega) = 4\pi^2 \delta(k_x - k_{pw,x}) \delta(\omega - \omega_{pw}) e^{-ik_{pw,y}y}. \quad (42)$$

A rectangular window is defined as

$$\Pi(x) = \begin{cases} 0 & \text{if } |x| > \frac{1}{2} \\ \frac{1}{2} & \text{if } |x| = \frac{1}{2} \\ 1 & \text{if } |x| < \frac{1}{2}. \end{cases} \quad (43)$$

The Fourier transform of a rectangular window with width  $(1/a)$  is given by [22]

$$\mathcal{F}_x\{\Pi(ax)\} := \frac{1}{|a|} \operatorname{sinc}\left(\frac{k_x}{2a}\right), \quad (44)$$

where  $\mathcal{F}_x\{\cdot\}$  relates a function to its Fourier transform with respect to  $x$ . The windowed sound field  $P_\Pi(x, y_{\text{ref}}, \omega)$  on the reference line in the  $k_x$ -space is given by convolving the desired plane wave with the transformed window function

$$\tilde{P}_\Pi(k_x, y_{\text{ref}}, \omega) = \frac{1}{|a|} \operatorname{sinc}\left(\frac{k_x}{2a}\right) *_{k_x} \tilde{P}(k_x, y_{\text{ref}}, \omega), \quad (45)$$

$$= \frac{4\pi^2}{|a|} \operatorname{sinc}\left(\frac{k_x - k_{pw,x}}{2a}\right) e^{-ik_{pw,y}y_{\text{ref}}} \delta(\omega - \omega_{pw}), \quad (46)$$

where  $*_{k_x}$  denotes a convolution with respect to  $k_x$ . Note that we formulated the plane wave using the complex exponential. Therefore, the spectrum of the convolution result will be one-sided unless  $\theta_{pw} = \pm\pi/2$  because then the relation  $k_x = k \cos(\theta_{pw}) = 0$  will hold.

In practice, using real-valued signals, the following expressions of the spectra will be two-sided. A convolution in the wavenumber domain  $k_x$  causes a spectral spread. A complex plane wave corresponds to a Dirac impulse in the wave number domain.

The spectrum of the convolution of such a Dirac impulse with a one dimensional, real valued function with a cutoff frequency of  $k_{c,x}$  is between  $k_{pw,x} - k_{c,x}$  and  $k_{pw,x} + k_{c,x}$ . The resulting one-dimensional function has a time dependency only in its the amplitude. The proof of the following lemma illustrate in a constructive manner the synthesis of one-dimensional sound figures by incorporating traveling waves only.

**Lemma:** A windowed wave function of the form

$$d_{\omega_{pw}}(x, t) = f(x) \cdot e^{-ik_{pw,x}x} \cdot e^{-ik_{pw,y}y_{ref}} \cdot e^{i\omega_{pw}t} \quad (47)$$

can be written in terms of monochromatic traveling waves, if the one dimensional real valued function  $f(x)$  has a cutoff frequency  $k_g$  such that  $k_{pw,x} + k_g \leq \frac{\omega_{pw}}{c}$ .

**Proof:** Since  $f(x)$  has been assumed to be bandlimited, it can be written as

$$\underbrace{f(x) \cdot e^{ik_{pw,x}x}}_{:=f_{\text{mod}}(x)} = \frac{1}{2\pi} \int_{-k_c+k_{pw,x}}^{k_c+k_{pw,x}} \tilde{F}(k_x - k_{pw,x}) e^{ik_x x} dk_x, \quad (48)$$

where  $\tilde{F}(k_x)$  denotes its Fourier transformation along the  $x$ -axis. For traveling waves, the requirement is to excite only monochromatic plane waves with the temporal frequency  $\omega_{pw}$  [34]. By exploiting the relation  $k_x = \frac{\omega_{pw}}{c} \cos(\theta)$ , defining  $\theta := \arccos\left(\frac{k}{\frac{\omega_{pw}}{c}}\right)$ , and if  $k_{pw,x} + k \leq \frac{\omega_{pw}}{c}$ , (48) can be reformulated as

$$f_{\text{mod}}(x) = \frac{1}{2\pi} \int_{-\pi}^{\pi} \tilde{F}(k(\cos(\theta) - \cos(\theta_{pw}))) e^{i\frac{\omega_{pw}}{c} \cos(\theta)x} d\left(\frac{\omega_{pw}}{c} \cos(\theta)\right). \quad (49)$$

By substituting this integral in (47) we get the windowed wave on the reference line in terms of traveling plane waves.

In Fig. 8 we illustrate the process of the back projection from the  $k_x$ -space (the spectrum of the one dimensional function is presented as a triangle<sup>4</sup>) onto the circle representing the 2-dimensional traveling plane waves with a specific  $k$ -number as performed by Eq. (49).

#### 5.4 Sound Figures as Functions on Two-Dimensional Manifolds

The discussion of the synthesis of 1-dimensional sound figures can be straightforwardly extended to cover the synthesis of periodic 2-dimensional figures of the temporal frequency  $\omega$  on a plane of interest,  $[x, y, 0]$ , using a 3-dimensional distribution of secondary sources such as, spherical or enclosing piecewise planar arrays.

We assume the figure is periodic and band limited. Otherwise we consider its band limited periodic continuation such that its spectrum is a discrete set  $\{(k_x, k_y) | (k_x, k_y) \in \mathbb{R}^2, \text{ and } k_x^2 + k_y^2 < (\frac{\omega}{c})^2\}$ . Analogously to Sect. 5.3, the cross section of a 3-dimensional plane wave with

<sup>4</sup> Note that the triangle does not represent the dependency between  $k_x$  and  $k_y$  but should exemplary reference to the general complex amplitude of the spectrum.

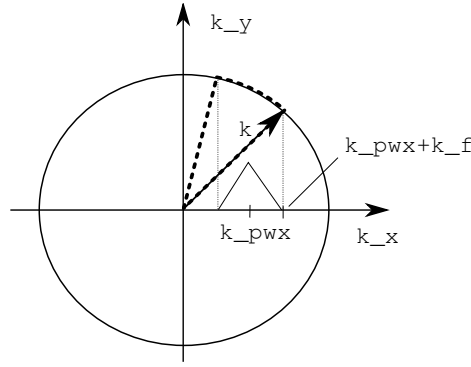


**Fig. 8** Illustration of the  $k$ -space.  $\mathbf{k}_{pw}$  denotes the wave vector of a traveling two-dimensional plane wave. The cutoff frequency of the one-dimensional function is denoted by  $k_g$ .  $k_{pw}$  denotes the wave number of the desired plane wave. Synthesizable traveling plane waves lie on the circle. The projection of the dotted arc on the  $k_x$ -axis is equivalent to the measured plane wave on a line that is parallel to the secondary source distribution.

a wave number  $k = \frac{\omega}{c}$  and angle of incidence  $[\varphi, \theta]$  represents a 2-dimensional plane wave with  $\mathbf{k} = [k_x, k_y] = [k \sin(\theta) \cos(\varphi), k \sin(\theta) \sin(\varphi)]$ . See Fig. 9.

Hence, for each element  $(k_x, k_y)$  belonging to the spectrum of the figure we synthesize a plane wave with angle of incidence according to

$$\theta = \arcsin \left( \sqrt{\frac{k_x^2 + k_y^2}{k^2}} \right), \quad (50)$$

and we choose a  $\varphi \in [0, 2\pi]$  such that

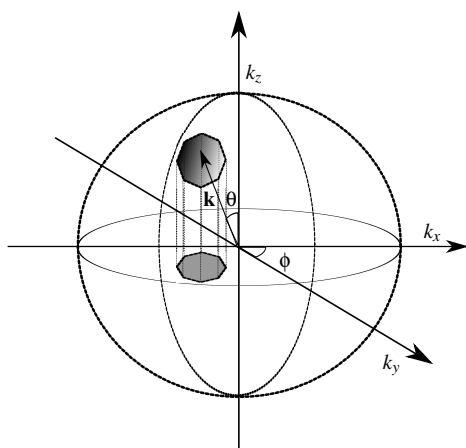
$$\frac{k_x}{k \sin(\theta)} = \cos(\varphi) \wedge \frac{k_y}{k \sin(\theta)} = \sin(\varphi). \quad (51)$$

Figure 9 represents the  $k$ -sphere for fixed temporal frequency  $\omega = k \cdot c$ . The 2-dimensional Fourier spectrum of a band limited two dimensional figure is exemplary restricted to an octagon in the  $k_x$ - $k_y$ -plane. Using Eq. (50) each point of the 2-dimensional spectrum is back projected to a point on the  $k$ -sphere corresponding to a traveling plane wave with the wave number  $k$  and a specific angle of incidence.

Hence, for the synthesis of a sound figure using a planar array, a 2-dimensional discrete Fourier transformation (DFT) for the desired figure is performed and the spectrum is convolved with the desired monochromatic frequency. The convolution result is then interpreted as a set of 3-dimensional plane waves with a single frequency but from different angles of incidence. The driving functions can then be computed in the  $k$ -space as outlined above and finally, an inverse two-dimensional Fourier transformation is performed to obtain the driving functions of each loudspeaker. In Fig. 10 we present a block diagram of the overall system for the synthesis of 2-dimensional sound figures.

## 6 Simulations and Discussion of Practical Aspects

To illustrate the theoretical derivations given so far, we present numeric simulations of the synthesized sound fields. We simulated a linear array of 50 omnidirectional loudspeakers,



**Fig. 9** k-space illustration for the synthesis of 2-dimensional sound figure. This figure generalizes Fig. 8 to the 3-dimensional case. Again, traveling plane waves are on the sphere, the projection of a point on the sphere on the  $k_x - k_y$ -plane is equivalent to a 3-dimensional plane wave measured by a plane.

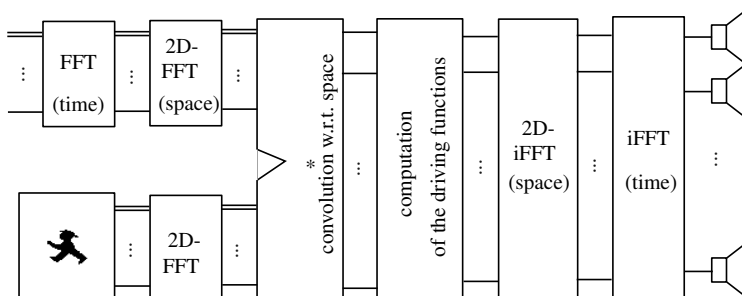


**Fig. 10** Block diagram of the proposed system for 2-dimensional sound figure synthesis using surrounding planar arrays. The manikin represents a desired sound figure.

separated by 15 cm, the spatial window chosen as a Hann-window [22] and, the desired sound field is a plane wave, whose angle of incidence is  $\pi/2$  with respect to the x-axis. The frequency is 800 Hz.

In Fig. 11 the real part of the synthesized sound field and its level distribution are depicted. To show the frequency dependent performance of the represented approach we computed the attenuation of the sound field at a point outside the desired sound field  $\mathbf{x} = [2\text{ m}, 1\text{ m}, 0]$  with respect to the point  $\mathbf{x} = [0\text{ m}, 1\text{ m}, 0]$  over the frequencies 20...2500 Hz. The result is given in Fig. 12. The curve shows that the attenuation begins to decrease after passing a particular frequency which can be understood as the aliasing frequency of the spatially discretized secondary source distribution.

In Fig. 13 we simulated a sound figure (tree leave) using a 3-dimensional setup of 6 planar arrays enclosing a volume of  $6 \times 6 \times 6\text{ m}$ . The depicted cross section of the simulated sound field is the plane of interest ( $z = 0$ ). Here again, we notice the high contrast achieved between the zone of quiet and the bright zone with the boundary of a tree leave.

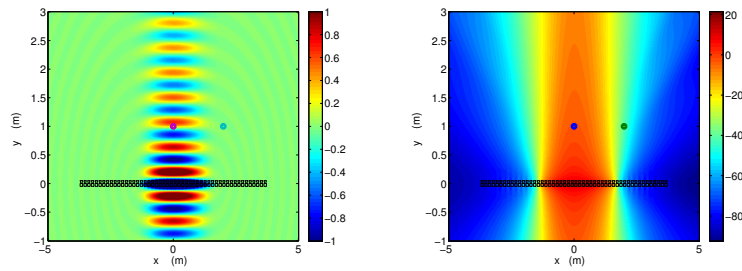


**Fig. 11** Linear array of 50 omnidirectional loudspeakers, separated by 15 cm synthesizing a windowed plane wave at a frequency of 800 Hz. The achieved level distribution is represented in [dB] and is shown on the right side.

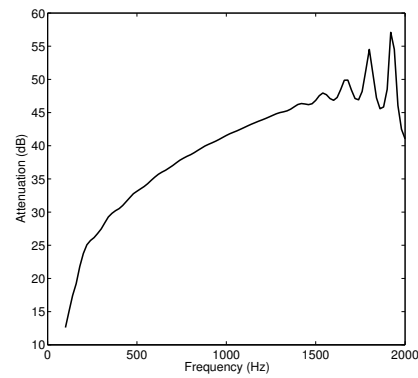


**Fig. 12** Overall attenuation of the sound field synthesized by a linear array of 50 loudspeakers at two different positions within and outside of the zone of quiet.

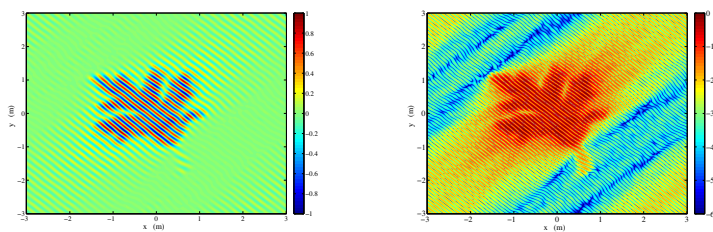


**Fig. 13** Synthesized sound field (left) and its level distribution in [dB] (right) using 6 planar arrays enclosing the listening room. Each of the arrays has  $40 \times 40$  elements with a spacing 15 cm.

## 6.1 Limitations on the Synthesis of Sound Figures

### 6.1.1 Reproduction in a Plane

As mentioned in Sect. 5.1 applying WFS or NFC-HOA on circular or WFS on rectangular arrays offers the desired reproduction of plane waves only in the plane of the array. In real-

world applications using one-dimensional arrays, the monopole sources approximated by loudspeakers cannot be considered as two-dimensional monopole sources. On the other hand they are used to synthesize a sound field in a plane. This is referred to as  $2\frac{1}{2}$ -dimensional synthesis [31]. Therefore, better results can be obtained, e.g., by using rectangular line or spherical loudspeaker arrays. Rectangular arrays with line loudspeakers can be understood as in-phase vertically layered rectangular arrays. The secondary sources of the different layers are identically driven according to Sect. 5.3. Such arrays extend the validity region of the synthesis.

To illustrate this, we simulated a window function on a line which is parallel to the synthesis array of 3-dimensional point sources as in Fig. 11 and in Fig. 14 we show the attenuation with respect to the height  $z$ .

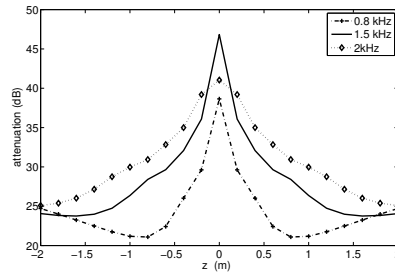


**Fig. 14** Achievable suppression depending on the  $z$ -coordinate and the frequency using a 50 elements linear array of point sources (2.5 dimensional synthesis). The attenuation is relative to the level of the sound field at the point  $[0\ 1\ 0]$  m.

### 6.1.2 Limitations due to Sampling Artifacts

Practical systems are realized by a finite number of loudspeakers. With increasing frequency this spatial sampling introduces increasing artifacts similar to the aliasing known from sampling a time signal. Hence, in order to keep the synthesis artifacts below a certain bound, the controllability of the sound field is available only up to a given frequency.

## 6.2 Robustness Due to Practical Aspects

In real-world applications the loudspeakers employed in an array exhibit individual characteristics which manifest amongst others in gain and phase mismatch. In the following we show by simulations, the consequences of such mismatches.

### 6.2.1 Loudspeaker Positioning Inaccuracy

So far, the secondary sources were considered to be identical. Loudspeakers could exhibit linear phase mismatch which is equivalent to a position mismatch such that in the case of a linear array the loudspeakers are not ideally aligned. We simulated positioning errors by introducing 2-dimensional normally distributed noise to the positions of the secondary sources, see Fig. 15. In Fig. 16 we show the synthesized sound field and its energy dis-



**Fig. 15** Radius of positioning mismatch was modeled as a 2-dimensional normal distributed process.

tribution with the window function, as used in Sect.5.3, and a variance of the positioning inaccuracy of  $\sqrt{(5\text{mm})^2 + (5\text{mm})^2}$ . To illustrate the influence of the positioning error over

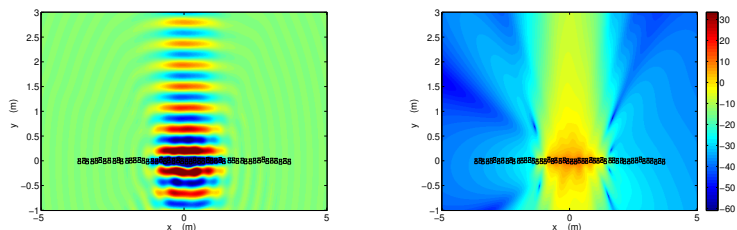


**Fig. 16** Sound field and its energy distribution at 800 Hz for a linear array with a spacing of 15 cm. The variance of the positioning tolerance is  $\sqrt{(5\text{mm})^2 + (5\text{mm})^2}$ . The achieved level distribution is represented in [dB] and is shown on the right side.

the frequency we present in Fig. 17 the achieved relative suppression between the two points used in Fig. 12. The simulations show that creating zones of quiet is highly sensitive to posi-

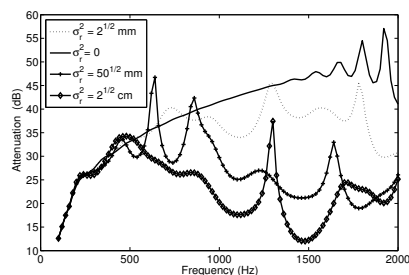


**Fig. 17** Achievable suppression over the frequency for different mismatch scenarios with a 50 elements linear loudspeaker array with a spacing of 15cm.

tioning and phase mismatches which is a consequence of the implicit differential mechanism employed in the synthesis.

### 6.2.2 Loudspeaker Gain Tolerance

The gain mismatch of the loudspeakers in a linear array was simulated by varying the gain of the individual loudspeakers. It was modeled as normally distributed process with zero mean and the variances 1/3 und 2/3 dB. The simulations in Fig. 18 show the sensitivity of the analytically derived driving functions to gain mismatches and emphasizes the importance of calibrating the loudspeakers used in an array for the synthesis of sound figures.

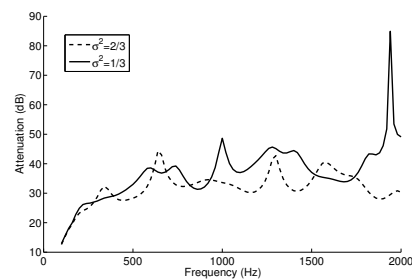


**Fig. 18** Achievable suppression over the frequency for different amplitude mismatch scenarios with a 50 elements linear loudspeaker array with a spacing of 15 cm. The mismatch was modeled as normal distributed process with the variances 1/3 and 2/3dB.

## 7 Conclusions

In this paper, we presented a versatile analytic formulation for the synthesis of sound fields with predefined areas of quiet. The approach stands to benefit from sound field synthesis techniques and their ability to synthesize arbitrary sound fields. The presented approach can be formulated in the frequency domain or time domain. Furthermore, it can be applied using arbitrary distributions of secondary sources on closed manifolds. A specialization to linear and arbitrary convex distributions is shown. The limitations of our approach are related to known limitations of conventional reproduction techniques such as WFS and NFC-HOA, namely, up to a predefined frequency the performance is limited by spatial sampling artifacts. The second limitation is referred to as the  $2\frac{1}{2}$ -dimensional synthesis problem. To prove our concept we performed numerical simulations including practical aspects, and have given some important design rules.

**Acknowledgements** We thank the reviewers for their thorough reading of the manuscript and highly appreciate the comments and suggestions.

## References

1. Abhayapala, T., Wu, Y.: Spatial soundfield reproduction with zones of quiet. In: 127th Audio Engineering Society Convention, New York, USA (2009)
2. Ahrens, J., Spors, S.: Sound field reproduction using planar and linear arrays of loudspeakers. *IEEE Transactions on Audio, Speech, and Language Processing* **18**(8), 2038–2050 (2010)
3. Arfken, G.: *Mathematical methods for physicists*, 6th edn. Elsevier, Boston (2005)
4. Berkhout, A.: *Applied seismic wave theory*. Elsevier Science (1987)
5. Berkhout, A., De Vries, D., Vogel, P.: Acoustic control by wave field synthesis. *The Journal of the Acoustical Society of America (JASA)* **93**, 2764–2778 (1993)
6. Berkhout, A., Wapenaar, C.: One-way versions of the Kirchhoff integral. *Geophysics* **54**(4), 460–467 (1989)
7. Boothby, W.M.: *An introduction to differentiable manifolds and Riemannian geometry*. Academic Press (1975)
8. Choi, J., Kim, Y.: Generation of an acoustically bright zone with an illuminated region using multiple sources. *Journal of the Acoustical Society of America (JASA)* **111**, 1695–1700 (2002)
9. Chung, F.: *Spectral graph theory*. Conference Board of the Mathematical Sciences. American Mathematical Society (1997)
10. Courant, D., Hilbert, R.: *Methods of Mathematical Physics*. Interscience Publishers Inc. (1953)
11. Daniel, J.: *Représentation de champs acoustiques, application à la transmission et à la reproduction de scènes sonores complexes dans un contexte multimédia*. Ph.D. thesis, Université Paris 6 (2000)

12. Fazi, F.: Sound field reproduction. Ph.D. thesis, University of Southampton, UK (2010). URL <http://eprints.soton.ac.uk/158639/>
13. Fazi, F., Nelson, P.: Sound field reproduction with an array of loudspeakers. *Rivista Italiana di Acustica* **35**(1) (2011)
14. Fazi, F., Nelson, P.A., Potthast, R.: Analogies and differences between three methods for sound field reproduction. In: 1st Ambisonic Symposium, Graz, Austria (2009)
15. Giroire, J.: Integral equation methods for the helmholtz equation. *Integral Equations and Operator Theory* **5**(1), 506–517 (1982)
16. Golub, G., Van Loan, C.: *Matrix computations*, 3rd edn. Johns Hopkins University Press, Baltimore (1996)
17. Gumerov, N.A., Duraiswami, R.: *Fast multipole methods for the Helmholtz equation in three dimensions*. Elsevier, Amsterdam (2004)
18. Helwani, K., Spors, S., Buchner, H.: Spatio-temporal signal preprocessing for multichannel acoustic echo cancellation. In: *Proc. IEEE Int. Conf. on Acoustics, Speech, and Signal Processing (ICASSP)* (2011)
19. Kleinberg, J., Tardos, E.: *Algorithm Design*. Addison-Wesley (2005)
20. Lanczos, C.: *Linear differential operators*. Courier Dover Publications (1997)
21. Menzies, D.: Sound field synthesis with distributed modal constraints. *Acta Acustica united with Acustica* **98**(1), 15–27 (2012)
22. Oppenheim, A.: *Discrete-time signal processing*, 2nd ed. edn. Prentice-Hall, Upper Saddle River N.J. (1999)
23. Poletti, M., Abhayapala, T.: Interior and exterior sound field control using general two-dimensional first-order sources. *The Journal of the Acoustical Society of America (JASA)* **129**(1), 234–244 (2011)
24. Poletti, M.A.: A unified theory of horizontal holographic sound. *J. Audio Eng. Soc.* **48**(12), 1155–1182 (2000)
25. Rabenstein, R., Steffen, P., Spors, S.: Representation of two-dimensional wave fields by multidimensional signals. *Signal Processing* **86**(6), 1341–1351 (2006)
26. Rosenberg, S.: *The Laplacian on a Riemannian Manifold: An Introduction to Analysis on Manifolds*. Cambridge University Press (1997)
27. Rossing, T.D.: *Springer Handbook of Acoustics*. Springer (2007)
28. Shin, M., Lee, S., Fazi, F., Nelson, P., Kim, D., Wang, S., Park, K., Seo, J.: Maximization of acoustic energy difference between two spaces. *The Journal of the Acoustical Society of America (JASA)* **128**, 121–131 (2010)
29. Spors, S.: Extension of an analytic secondary source selection criterion for wave field synthesis. In: 123th Audio Engineering Society Convention, New York, USA (2007)
30. Spors, S., Helwani, K., Ahrens, J.: Local sound field synthesis by virtual acoustic scattering and Time-Reversal. In: 131st Audio Engineering Society Convention, New York, USA
31. Spors, S., Rabenstein, R., Ahrens, J.: The theory of wave field synthesis revisited. 124th Audio Engineering Society Convention, Amsterdam, Netherlands **124** (2008)
32. Teutsch, H.: *Modal array signal processing: principles and applications of acoustic wavefield decomposition*. Springer Verlag (2007)
33. Tikhonov, A., Samarskii, A.: *Equations of Mathematical Physics*. Dover Publications (1963)
34. Williams, E.: *Fourier acoustics: sound radiation and nearfield acoustical holography*. Academic Press (1999)
35. Zotter, F., Spors, S.: Is sound field control determined at all frequencies? how is it related to numerical acoustics? In: *Audio Engineering Society Conference: 52nd International Conference*, pp. 1–9. Guildford, UK (2013)